Detecting and Diagnosing Process Nonlinearity-Induced Unit-Wide Oscillations Based on an Optimized Multivariate Variational Mode Decomposition Method

ZHULIANG LIN[1], MIN SUN[2], AND XIALAI WU[ID][3]
[1]Xingzhi College, Zhejiang Normal University, Lanxi 321017, China
[2]Zhejiang Kende Mechanical and Electrical Company Ltd., Taizhou 318050, China
[3]School of Engineering, Huzhou University, Huzhou, Zhejiang 313000, China

Corresponding author: Xialai Wu (xlaihzh@126.com)

ABSTRACT In process control system, nonlinearity-induced unit-wide oscillations are a common fault, which degrades the control performance and threaten the stability. It is important to detect and diagnose the nonlinearity-induced unit-wide oscillations to improve the process control performance. In this paper, a novel method, termed as SSA-MVMD, is proposed by combining the sparrow search algorithm (SSA) and multivariate variational mode decomposition (MVMD) to detect and diagnose the nonlinearity-induced unit-wide oscillations. MVMD is an advanced signal decomposition and time-frequency method. However, its performance is affected by the mode number K and penalty coefficient α. SSA is adopted to optimize the parameters of MVMD. Then, a novel SSA-MVMD-based detector is presented to detect and diagnose the nonlinearity-induced unit-wide oscillations. The proposed method is model-free and data-driven thus requiring no prior knowledge about the process dynamics. Compared with the latest related works, the proposed method can better decompose the multivariate nonstationary signals and adaptively analyze the unit-wide oscillations. In the end, the effectiveness and advantages are demonstrated by simulations as well as industrial cases.

INDEX TERMS Oscillation detection, multivariate variational mode decomposition, signal decomposition, control performance assessment.

I. INTRODUCTION

Oscillations in the process control system are a very common problem [1]. The existence of oscillation in the control loop increases the deviation from the set value of process variables, resulting in poor quality products, larger rejection rate, increased energy consumption and reduced average throughput. There are several reasons for the oscillation in the control loop. They may be caused by excessive controller gain or external disturbance, but a more common cause of oscillation is valve stiction, which is the most typical nonlinear fault in process control system [2], [3]. Due to the interconnection between loops, the oscillation generated by one control loop

is easy to be transmitted to other loops to form unit-wide oscillations [4]. Therefore, the motivation of this work is to detect and diagnose the nonlinearity-induced unit-wide oscillations in the process control system to improve the safety and economy.

Unit-wide oscillation detection and diagnosis technology has been developed for more than twenty years [5]. A direct idea for unit-wide oscillation detection is to detect each control loop one by one through using the single-loop oscillation analysis methods, such as integral absolute error (IAE) [6], zero-crossing [7], auto-covariance function (ACF) [8], autoregressive moving average model [9], and so on. However, these methods have the shortcoming of not considering the connectivity of the control loops. In fact, control loops are not isolated from each other. Specifically,

---

The associate editor coordinating the review of this manuscript and approving it for publication was Francesco Tedesco[ID].

the reason for oscillation of a control loop may be that it is interfered by disturbance from other loops. Therefore, it is necessary to use multivariate analysis technology to detect and diagnose unit-wide oscillations.

Recently, with the development of signal processing technology, signal decomposition methods are widely used in oscillation detection and diagnose, because these methods are able to process nonlinear and nonstationary signals. Signal processing methods have been used in many engineering fields, such as motor bearing fault detection [10] and cognitive computing [11]. The research on process oscillation detection and diagnosis mainly used signal decomposition methods. Srinivasan *et al.* [12] proposed a modified empirical mode decomposition (EMD) method to detect the process oscillations. Following, the local mean decomposition (LMD) [13], intrinsic time-scale decomposition (ITD) [14], [15], and variational mode decomposition (VMD) [16] are utilized to analyze specific types of oscillations in succession.

However, the univariate signal decomposition method is not suitable for processing multivariate signals, because multivariate signal decomposition has two requirements [17]: (i) alignment of frequency information across multiple channels in each mode, termed as mode-alignment; (ii) incorporating any correlation between multiple data channels. The most straightforward method for multivariate signal processing is analyzing each channel of a multivariate signal separately using univariate signal processing techniques. In this way, the results would not fulfill the above requirements, because the mutual relationships among channels are not considered [18].

Lang *et al.* [19] pioneered the use of multivariate empirical mode decomposition (MEMD) [20] for detecting unit-wide oscillations. Then, Aftab *et al.* [21] further utilized the MEMD and its noise-assisted version, namely NA-MEMD [22], to detect and diagnose the unit-wide oscillations. Due to the low computational efficiency of MEMD, Lang *et al.* [23] proposed a fast MEMD (FMEMD) algorithm to reduce the computational complexity. Later, the FMEMD algorithm is adopted to monitoring unit-wide oscillations in noisy process [24]. Apart from MEMD class methods, Lang *et al.* developed the indirect and direct multivariate intrinsic time-scale decomposition, namely IMITD [25] and DMITD [26], to analyze the unit-wide oscillations. The above multivariate signal decomposition-based methods consider the multivariate relationship of unit-wide oscillations, but signal decomposition methods are empirical in themselves and lack of theoretical basis. In addition, the performance of these multivariate signal decomposition methods depends on the direction and number of projection vectors, which is an unsolved problem.

More recently, Rehman and Aftab [17] proposed the multivariate variational mode decomposition (MVMD) algorithm, which is based on mathematical optimization theory and outperforms the MEMD in noisy environment. At present, MVMD has been applied in biomedical

signal processing [27], time series prediction [28], and so on. The MVMD-based unit-wide oscillation detection and diagnosis has not been reported. Therefore, this paper aims to use the MVMD to detect and diagnosis the unit-wide oscillations in process industries. Although MVMD shows attractive properties, its performance relies on the selection of mode number and penalty coefficient. At present, there are few reports on this issue.

To tackle this issue, this paper utilizes the sparrow search algorithm (SSA) [29] to search the optimal parameters of MVMD, thus an SSA-MVMD algorithm is successfully proposed. The SSA-MVMD algorithm can adaptively decompose the complex unit-wide oscillations into a series of modes and provide the corresponding center frequencies. Based on the decomposition results, a novel oscillation detector is developed by combining the normalized correlation coefficient and sparseness index, which is able to automatically identify significant oscillating modes. Enlightened by the fact that the nonlinearity-induced oscillations contain higher order harmonics [30], thus the presence of harmonics can be used as an indicator of nonlinearity problems. Following, a process nonlinearity-induced unit-wide oscillation diagnosis method is proposed through calculating the oscillation frequency relationship among modes. Although SSA and MVMD have been applied in other fields respectively, there is no report on the joint use of these two methods in process oscillation detection and diagnosis. Therefore, the proposed method is novel, and its application to detecting and diagnosing nonlinearity-induced unit-wide oscillations also enriches and improves the control system monitoring performance. The contributions of this work are as follows,

(i) An SSA-MVMD algorithm is proposed to improve the performance of the basic MVMD algorithm. In addition, the proposed method also outperforms MEMD, IMITD, DMITD, and MNCMD in decomposition performance;

(ii) A novel SSA-MVMD-based oscillation detector is developed by combining the normalized correlation coefficient and sparseness index to identify the significant oscillating modes of process variables;

(iii) A novel nonlinearity-induced unit-wide oscillation diagnosis strategy is presented through investigating the oscillating frequency relationship among different modes;

(iv) Compared with the existing works, such as MEMD-based or MITD-based methods, the proposed method shows better adaptability and decomposition performance, thus providing more accurate and reliable detection and diagnosis results.

This paper hereafter is organized as follows. The multivariate variational mode decomposition and sparrow search algorithm are briefly introduced in Section II. The proposed method is elaborated in Section III, which includes SSA-MVMD algorithm and its application in detecting and diagnosing oscillations. Simulations and industrial cases are provided in Section IV and V, respectively, followed by conclusions.

II. PRELIMINARIES
A. MULTIVARIATE VARIATIONAL MODE DECOMPOSITION
MVMD is a nature multivariate extension of univariate VMD [17]. It first defines the multivariate mode, which is expressed in a vector form,

$$\mathbf{u}_{k,q}(t) = \begin{bmatrix} u_{k,1} \\ u_{k,2} \\ \vdots \\ u_{k,Q} \end{bmatrix} = \begin{bmatrix} a_{k,1} \\ a_{k,2} \\ \vdots \\ a_{k,Q} \end{bmatrix} \cos(\varphi_k(t)) \quad (1)$$

where Q is the channel number. This definition considers the relationship between different channels of multivariate signals [31]. The original multivariate signals is $\mathbf{x}(t) = [x_1(t), x_2(t), \ldots, x_Q(t)]$, and

$$\mathbf{x}(t) = \sum_{k=1}^{K} \mathbf{u}_k(t) \quad (2)$$

where $\mathbf{u}_k(t) = [u_1(t), u_2(t), \ldots, u_Q(t)]$. Next, the analytic representation of the vector signal $\mathbf{u}_{k,q}(t)$ can be obtained by employing the Hilbert transform operator,

$$\mathbf{u}_{k,q}^A(t) = \mathbf{u}_{k,q}(t) + j\mathcal{H}\left(\mathbf{u}_{k,q}(t)\right)$$

$$= \begin{bmatrix} a_{k,1} \\ a_{k,2} \\ \vdots \\ a_{k,Q} \end{bmatrix} \exp(j\varphi_k(t)) \quad (3)$$

where $\mathcal{H}(\cdot)$ is Hilbert transform operator.

The goal of MVMD is to extract an ensemble of modes $\{\mathbf{u}_k(t)\}$, $k = 1, 2, \ldots, K$ in the input signal. These modes satisfy the conditions that (i) the sum of bandwidths of these modes is minimum and (ii) they can exactly reconstruct the original input data. To achieve this goal, the resulting cost function of MVMD is established as follows,

$$\min_{\{u_{k,q}(t)\},\{\omega_k\}} \left\{ \sum_{k=1}^{K} \sum_{q=1}^{Q} \left\| \partial_t \left[\mathbf{u}_{k,q}^A(t) \right] e^{-j\omega_k t} \right\|_2^2 \right\}$$

$$s.t. \sum_{k=1}^{K} u_{k,q}(t) = x_q(t), \quad q = 1, 2, \ldots, Q \quad (4)$$

The corresponding augmented Lagrangian function of this constrained optimization problem is

$$L = \alpha \sum_{k=1}^{K} \sum_{q=1}^{Q} \left\| \partial_t \left[\mathbf{u}_{k,q}^A(t) \right] e^{-j\omega_k t} \right\|_2^2$$

$$+ \sum_{q=1}^{Q} \left\| x_q(t) - \sum_{k=1}^{K} u_{k,q}(t) \right\|_2^2$$

$$+ \sum_{q=1}^{Q} \left\langle \lambda_q(t), x_q(t) - \sum_{k=1}^{K} u_{k,q}(t) \right\rangle \quad (5)$$

where α stands for the penalty coefficient; λ_q and $\langle \cdot, \cdot \rangle$ represent the Lagrangian multipliers and inner product, respectively.

The solution of the original optimization problem can be founded as the saddle point of the Lagrangian function, which is solved by ADMM (Alternating Direction Method of Multipliers) [17]. ADMM can disassemble the complete optimization problem into a sequence of iterative sub-optimization problems. MVMD can extract the modes and center frequencies by alternately updating the modes and center frequencies. The detailed algorithm can be found in reference [17]. It can be observed from (5) that MVMD requires users to specify the mode number K and penalty coefficient α in advance.

B. SPARROW SEARCH ALGORITHM
SSA is a new swarm intelligence optimization algorithm proposed in recent years [29]. It has the advantages of strong optimization, low restriction on objectives and less adjustment parameters. This algorithm has been successfully applied to some practical engineering fields, such as biomedical engineering [27], clutter filtering [32], and so on. At present, the application of SSA in unit-wide oscillation analysis has not been reported. Therefore, this paper proposes to use SSA to optimize the parameters of MVMD in order to improve the performance of unit-wide oscillation detection and diagnosis.

In SSA, the sparrow population is divided into two types, namely, producer and scrounger. For simplicity, the procedures of SSA are summarized as follows:

(i) Initialize sparrow population location, which is expressed as

$$S = \begin{bmatrix} s_{1,1} & s_{1,2} & \cdots & s_{1,\dim} \\ s_{2,1} & s_{2,2} & \cdots & s_{1,\dim} \\ \vdots & \vdots & \ddots & \vdots \\ s_{n,1} & s_{n,2} & \cdots & s_{n,\dim} \end{bmatrix} \quad (6)$$

where n is the number of sparrows and *dim* is the variable dimension of the problem to be optimized. The fitness value of the initial population can be obtained through the matrix,

$$f_s = \begin{bmatrix} f\left(\begin{bmatrix} s_{1,1} & s_{1,1} & \cdots & s_{1,\dim} \end{bmatrix}\right) \\ f\left(\begin{bmatrix} s_{2,1} & s_{2,2} & \cdots & s_{2,\dim} \end{bmatrix}\right) \\ \vdots \\ f\left(\begin{bmatrix} s_{n,1} & s_{n,2} & \cdots & s_{n,\dim} \end{bmatrix}\right) \end{bmatrix} \quad (7)$$

where f_s and f represent the fitness value and fitness function, respectively.

(ii) Producers in the population are responsible for finding the direction and location of food, and leading scroungers to approach the direction of food. Once a sparrow finds the trace of a predator, it will sound to warn the population. When the warning signal value is greater than the safety threshold, the producer will lead the whole population to move to the safe area. Therefore, the producer position in the population is updated as follows

$$S_{i,j}^{m+1} = \begin{cases} S_{i,j}^m \cdot e^{-\frac{1}{\vartheta \cdot M}}, & if \ R_2 < ST \\ S_{i,j}^m + G \cdot L, & if \ R_2 \geq ST \end{cases} \quad (8)$$

where m stands for the current iteration; M is a constant with the largest number of iterations; $\vartheta \in (0, 1]$ indicates a random number; $R_2 \in [0, 1]$ and $ST \in [0.5, 1.0]$ denotes warning signal value and safety threshold, respectively; G is a random number which obeys normal distribution; L shows a matrix of $1 \times d$ for which each element inside is 1.

(iii) When the fitness value of the producer's location is low, some hungry scroungers may move to other locations to get food. At the same time, scroungers will constantly monitor producers and then compete for food resources in oder to improve their predation rate. Therefore, the location of scrounger in the population is updated as follows

$$S_{i,j}^{m+1} = \begin{cases} G \cdot e^{-\frac{S_{worst} - S_{i,j}^{m}}{i^2}}, & \text{if } i > \frac{n}{2} \\ S_p^{m+1} + \left| S_{i,j}^{m} - S_{i,j}^{m+1} \right| \cdot A^+ \cdot L, & \text{if } i \leq \frac{n}{2} \end{cases} \quad (9)$$

where A stands for a matrix of $1 \times d$ for which each element inside is randomly assigned 1 or -1, and $A^+ = A^T \left(A A^T \right)^{-1}$; S_p is the optimal position occupied by the producer; S_{worst} represents the current global worst location.

(iv) When an individual in the population perceives danger, the individual at the edge will move towards the safe area, and the sparrow originally located in the center of the population will move randomly to form a new population, namely,

$$S_{i,j}^{m+1} = \begin{cases} S_{best}^{m} + \gamma \left| S_{i,j}^{m} - S_{best}^{m} \right|, & \text{if } f_i > f_g \\ S_{i,j}^{m} + \xi \frac{\left| S_{i,j}^{m} - S_{worst}^{m} \right|}{f_i - f_w + \varepsilon}, & \text{if } f_i = f_g \end{cases} \quad (10)$$

where S_{best}^{m} is the current global optimal location; γ represents the step size, which is a normal distribution of random numbers with a mean value of 0 and a variance of 1. f_i, f_g and f_w denote the fitness value of the present sparrow, the current global best and worst fitness values, respectively. ε is the smallest constant so as to avoid zero-division-error.

III. PROPOSED METHOD

MVMD is a promising multivariate signal processing tool. However, its performance relies on the selection of mode number K and penalty coefficient α. SSA is utilized in this section to search the optimal parameters of MVMD.

A. SSA-MVMD

It is necessary to define an appropriate objective function to optimize MVMD using SSA. Because MVMD is expected to decompose process variables into regular oscillations, the approximate entropy (AE) is adopted to measure the regularity. AE is mainly used to characterize the complexity of time series. It has the advantages of short points for calculating data, strong anti-noise and anti-interference ability. It is also applicable to both deterministic signals and random signals. More specifically, AE distinguishes various processes by calculating the edge probability distribution of time series.

It can quantitatively describe the randomness and irregularity of time series. The greater the complexity of the series, the larger the approximate entropy. The calculation process is shown in Algorithm 1.

Algorithm 1 Calculation Process of AE

1: Denote the decomposed mode as $u_{k,q}(t) = \{u(n)\} = \{u(1), u(2), \ldots u(N)\}$, where N is the data length;

2: Given a data pattern number τ in advance, the sequence is formed into an τ-dimensional vector $U_\tau(1), U_\tau(2), \ldots, U_\tau(N - \tau + 1)$, where

$$U_\tau(i) = \{u(i), u(i+1), \ldots, u(i + \tau - 1)\}; \quad (11)$$
$$i = 1, 2, \ldots, N - \tau + 1$$

3: Define the distance between vectors $U_\tau(i)$ and $U_\tau(j)$ as

$$d[U_\tau(i), U_\tau(j)] = \max_{\varsigma \in [0, \tau-1]} |u(i+\varsigma) - u(j+\varsigma)|; \quad (12)$$

4: Assume the similarity tolerance is r and count the number satisfying $d[U_\tau(i), U_\tau(j)] < r$, $U_\tau(j) (1 \leq j \leq N - \tau + 1)$. Denote the ratio of $num\{d[U_\tau(i), U_\tau(j)] < r\}$ and total number $N - \tau + 1$ as

$$B_i^{(\tau)}(r) = \frac{1}{N - \tau + 1} num\{d[U_\tau(i), U_\tau(j)] < r\}; \quad (13)$$

5: Calculate the logarithmic mean of $B_i^{(\tau)}(r)$,

$$B^{(\tau)}(r) = \frac{1}{N - \tau + 1} \sum_{i=1}^{N - \tau + 1} \ln B_i^{(\tau)}(r); \quad (14)$$

6: Increase the vector dimension to $m+1$ and repeat step 11 - 14 to obtain $B^{(\tau+1)}(r)$;

7: The approximate entropy is calculated as

$$AE = B^{(\tau+1)}(r) - B^{(\tau)}(r). \quad (15)$$

It can be seen from (15) that AE is a dimensionless scalar, and its value is related to τ and r. A large number of statistical results show that when $\tau = 2$ and $r = 0.2$, the AE has reasonable statistics [33].

AE can only measure the complexity of the mode itself, but cannot reflect the relationship between the mode $u_{k,q}(t)$ and the original signal $x_q(t)$. Therefore, the Pearson correlation coefficient (PCC) [16] is adopted,

$$\rho_{k,q} = \frac{Cov(x_q(t), u_{k,q}(t))}{\sqrt{Var(x_q(t)) Var(u_{k,q}(t))}} \quad (16)$$

where $Cov(\cdot, \cdot)$ and $Var(\cdot)$ represent the covariance and variance, respectively.

Herein, combining AE and PCC, this paper proposes a novel fitness function for SSA-MVMD, which is

expressed as

$$
\begin{cases}
fitness = \max \left\{ \sum_k \sum_q \dfrac{\rho_{k,q}}{AE_{k,q}} \right\} \\
s.t. \quad \alpha \in \left[10^{-1}, 10^5 \right] \\
\qquad K = 1, 2, \ldots, 15
\end{cases}
\tag{17}
$$

where k and q are mode index and channel index, respectively. The fitness function $\sum_k \sum_q \frac{\rho_{k,q}}{AE_{k,q}}$ comprehensively considers the complexity of the mode itself and the relationship with the original signal, which is used to quantitatively evaluate the decomposition performance. The optimal parameter pairs K and α of MVMD can be obtained by SSA. The procedures of SSA-MVMD are summarized in Algorithm 2.

Algorithm 2 MVMD-SSA

1: Initialize SSA parameters, such as maximum iterations and population number;
2: **while** $m < M$ **do**
3:     MVMD is performed for producers and scroungers in each location, and the initial fitness value is calculated;
4:     Update the producer location (Eq. (8)) according to the alarming value, and then update the scrounger location (Eq. (9));
5:     According to Eq. (10), update the location of sparrows that find predators;
6:     Update fitness values, best location, and worst location;
7: **end while**
8: Return the optimal parameters K and α.

B. DETECTING AND DIAGNOSING UNIT-WIDE OSCILLATIONS

After using SSA-MVMD to decompose process variables, the next step is to detect whether these modes are significantly oscillatory modes.

Firstly, because the spurious modes are weakly correlated with the original signal, correlation coefficients are commonly adopted to quantify this relationship. Herein, we use normalized correlation coefficient to eliminate spurious modes. The normalized correlation coefficient is calculated as,

$$
\varpi_{k,q} = \frac{\rho_{k,q}}{\max \left\{ \rho_{1,q}, \rho_{2,q}, \ldots, \rho_{K,q} \right\}}
\tag{18}
$$

Only modes with $\varpi_{k,q} > \widehat{\varpi}$ can be retained as significant components, where $\widehat{\varpi}$ denotes the threshold. $\widehat{\varpi} = 0.15$ is recommended by references [34]

Having selected the significant modes, the next task is to evaluate the oscillation degree of these modes, because there is no need to analyze the slightly oscillating modes [25]. For process oscillations, they often have obvious peaks in the spectrum, while the amplitudes at other frequencies are

---

Algorithm 3 MVMD-SSA-Based Detection and Diagnosis Method

Input: Process variables $\mathbf{x}(t) = \left[x_1(t), x_2(t), \ldots, x_Q(t) \right]$;
Output: Whether the unit-wide oscillation is induced by nonlinearity problems;
1: Decompose the multivariate signal $\mathbf{x}(t)$ using MVMD-SSA, which is detailed in Algorithm 2. Thus modes $u_{k,q}(t), k = 1, 2, \ldots, K, q = 1, 2, \ldots, Q$ can be obtained;
2: **for** $q = 1, 2, \ldots, Q$ **do**
3:     **for** $k = 1, 2, \ldots, K$ **do**
4:         Detect the oscillating modes according to the conditions $\varpi_{k,q} > \widehat{\varpi}$ and $\zeta_{k,q} > \widehat{\zeta}$;
5:     **end for**
6:     Assume there are D_q significant oscillating modes. For these modes, calculate their mean frequency, maximum frequency, and minimum frequency by (21), (22), and (23), respectively;
7:     **for** $i = 1, 2, \ldots, D_q$ **do**
8:         **if** $Min_f^j \leq zM_f^i \leq Max_f^j, i = 1, 2, \ldots, D_q, j \neq i$, and z is an integer **then**
9:             The z-th order harmonic is detected in the q-th variable/loop, which means the presence of nonlinearity-induced oscillations;
10:         **else**
11:             This variable/loop is not influenced by nonlinearity problems.
12:         **end if**
13:     **end for**
14: **end for**

---

very small. Therefore, the oscillation degree can be quantified by evaluating the sparsity of the spectrum vector. Sparseness index [12] is an ideal indicator to achieve this goal

$$
\zeta_{k,q} = \frac{\sqrt{N} - \dfrac{\sum_n |\hat{u}_{k,q}(n)|}{\sqrt{\sum_n |\hat{u}_{k,q}(n)|^2}}}{\sqrt{N} - 1}
\tag{19}
$$

where $\hat{u}_{k,q}(n)$ stands for the frequency response of mode $u_{k,q}(t)$; N is the vector length. $\zeta_{k,q}$ is a number between 0 and 1. The closer it is to 1, the more significant the oscillation degree is. According to references [5], [21], if $\zeta_{k,q} > \widehat{\zeta}$, where $\widehat{\zeta} = 0.58$, the corresponding mode can be regraded to be oscillatory.

When the oscillations are detected, they can be diagnosed whether the oscillation is caused by nonlinearity problem. Inspired by the idea that oscillations caused by nonlinearities contain higher order harmonics [35], this paper presents an SSA-MVMD-based strategy to diagnose the unit-wide oscillations by investigating the oscillation period relationship among different modes. More specifically, if $\Delta t_{k,q}$ represents the time interval between two successive zero crossings of the significant oscillating mode, then the average time $\bar{P}$
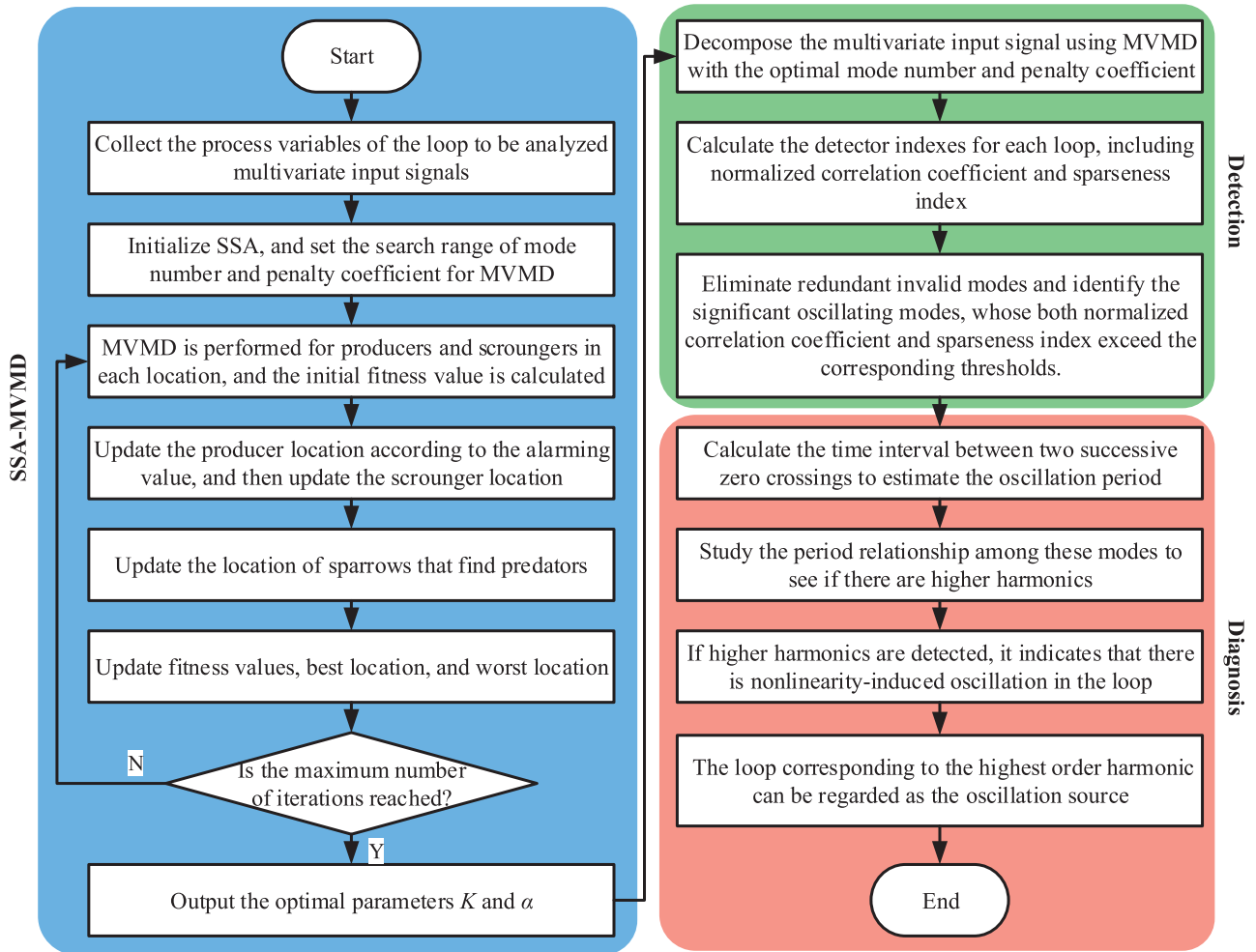
FIGURE 1. The proposed workflow for detecting and diagnosing the nonlinearity-induced unit-wide oscillations based on the SSA-MVMD algorithm.

for $I = 11$ such intervals will be given by [5]

$$\bar{P}_{k,q} = \frac{2\sum_{i=1}^{I} \Delta t_{k,q}^{(i)}}{I} \qquad (20)$$

The corresponding mean frequency, maximum frequency, and minimum frequency are

$$M_f = \frac{1}{\bar{P}} \qquad (21)$$

$$Max_f = \frac{1}{\bar{P} - Std\,(\Delta t)} \qquad (22)$$

$$Min_f = \frac{1}{\bar{P} + Std\,(\Delta t)} \qquad (23)$$

respectively, where $Std\,(\Delta t)$ is the standard deviation of the time intervals between zero crossings. The presence of harmonics is established if there exists mean time periods of modes that are integral multiples.

The detection and diagnosis steps are listed in Algorithm 3. The complete flow of the proposed method is shown in
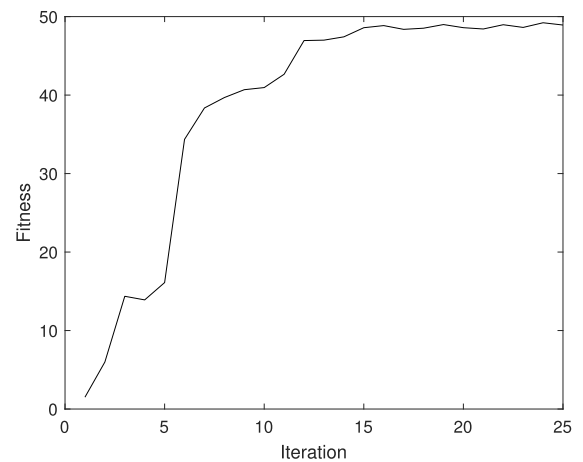
FIGURE 2. The SSA fitness curve for MVMD parameter optimization process. It can be observed that this curve shows a trend of convergence.

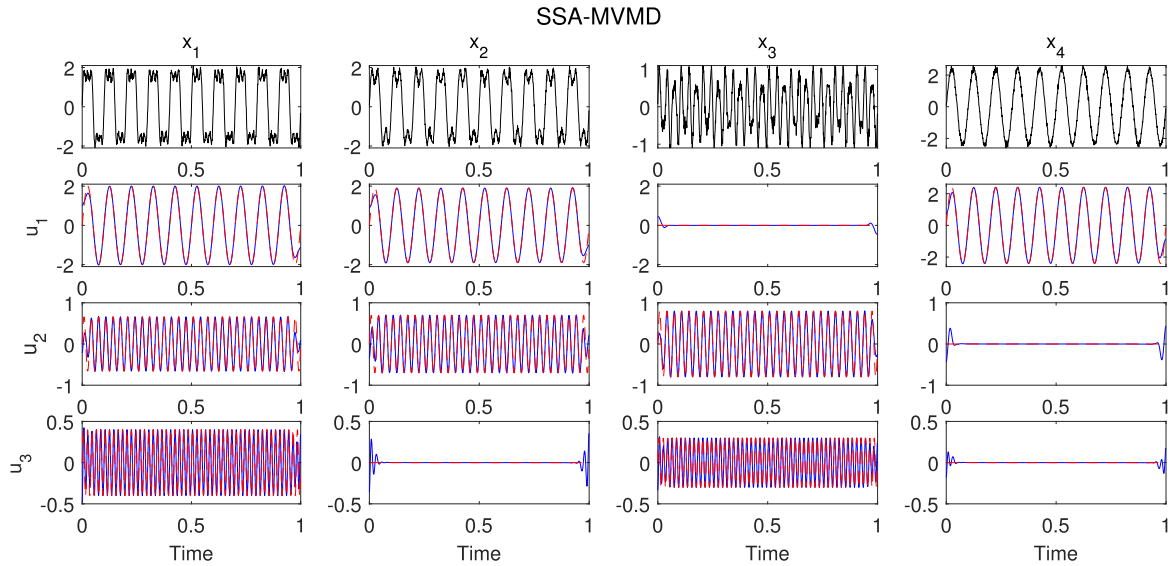Figure 1, which includes SSA-MVMD algorithm, oscillation detection and diagnosis.

SSA-MVMD

FIGURE 3. The decomposition results of SSA-MVMD. The black line indicates the input signal. The blue solid line and the red dotted line represent the decomposed mode and the actual mode respectively. It can be seen that the blue lines and the red lines basically coincide, which indicates that the mode extraction is correct.
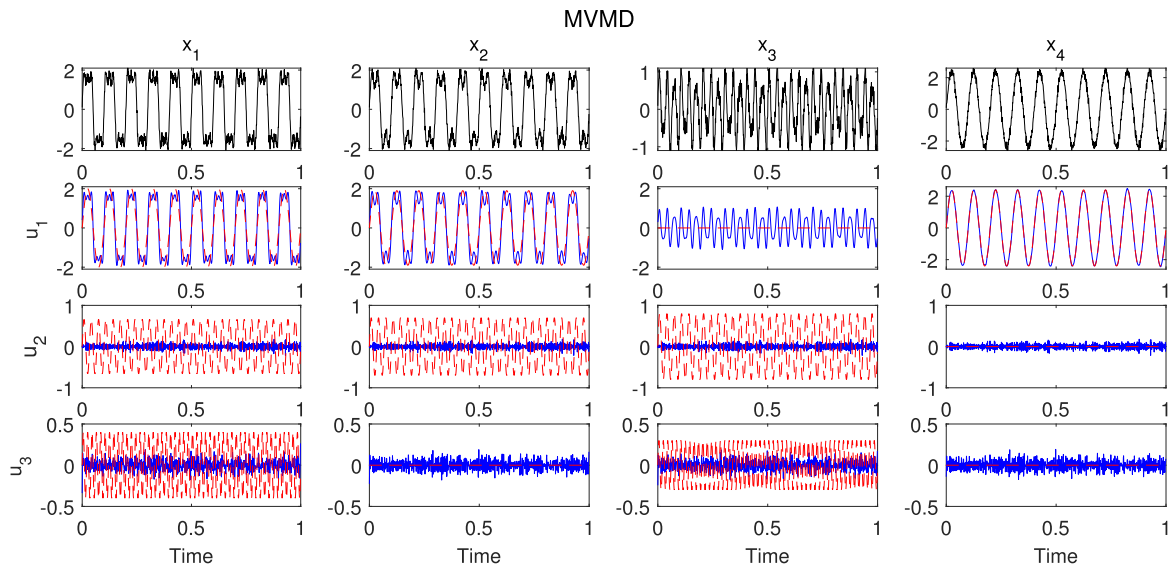
MVMD

FIGURE 4. The decomposition results of MVMD without optimizing the α parameter. The blue solid line and the red dotted line represent the decomposed mode and the actual mode respectively. It can be seen that the MVMD cannot properly decompose the signal under this condition.

Remark 1: The proposed method aims to use SSA to optimize the parameter pair of MVMD. Therefore, its complexity is mainly composed of SSA and MVMD. Both SSA and MVMD are very new. However, the rigorous complexity analysis of SSA and MVMD has not been reported. This problem is beyond the scope of this study and we would like to investigate the complexity of SSA and MVMD in the future. In this paper, we focus on detecting and diagnosing the process nonlinearity-induced unit-wide oscillations. This task is completed off-line and does not require on-line implementation, so the requirement for complexity is not high. The existing reference [29] shows that SSA is a new fast convergence

algorithm. This is one of the reasons why we choose this optimization algorithm. In all cases, the proposed method can complete the operations (including optimization, decomposition, detection and diagnosis) in less than half a minute. This time complexity is sufficient to meet the needs of process oscillation detection and diagnosis [34].

IV. SIMULATIONS
In this section, a numerical case and a control system are investigated to test the effectiveness and advantages of the proposed method.
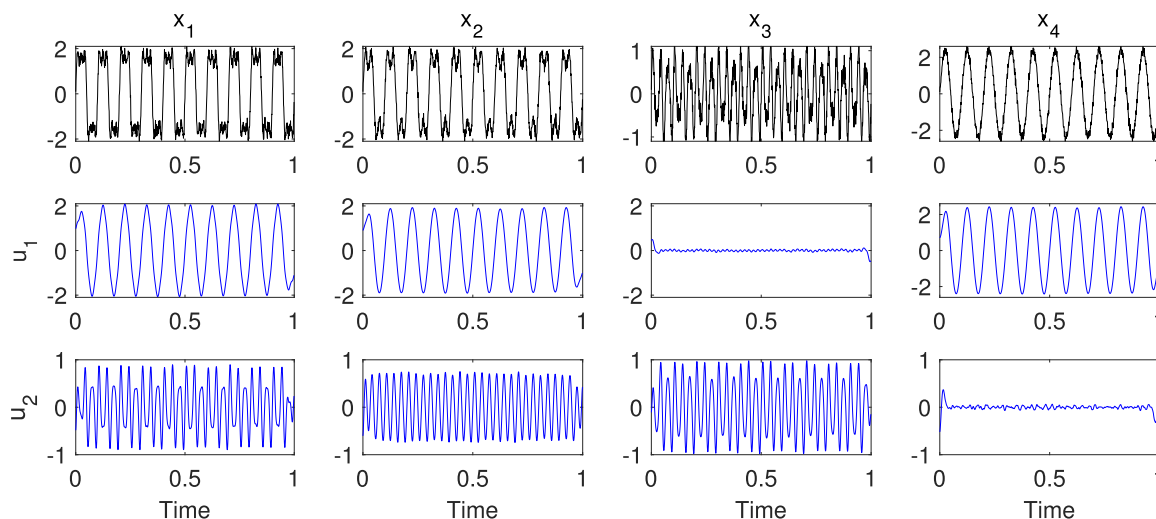
FIGURE 5. The decomposition results of MVMD with $K = 2$, which is subjected to under-decomposition issue [36]. The black line and the blue line represent the input signal and the decomposed signal, respectively.
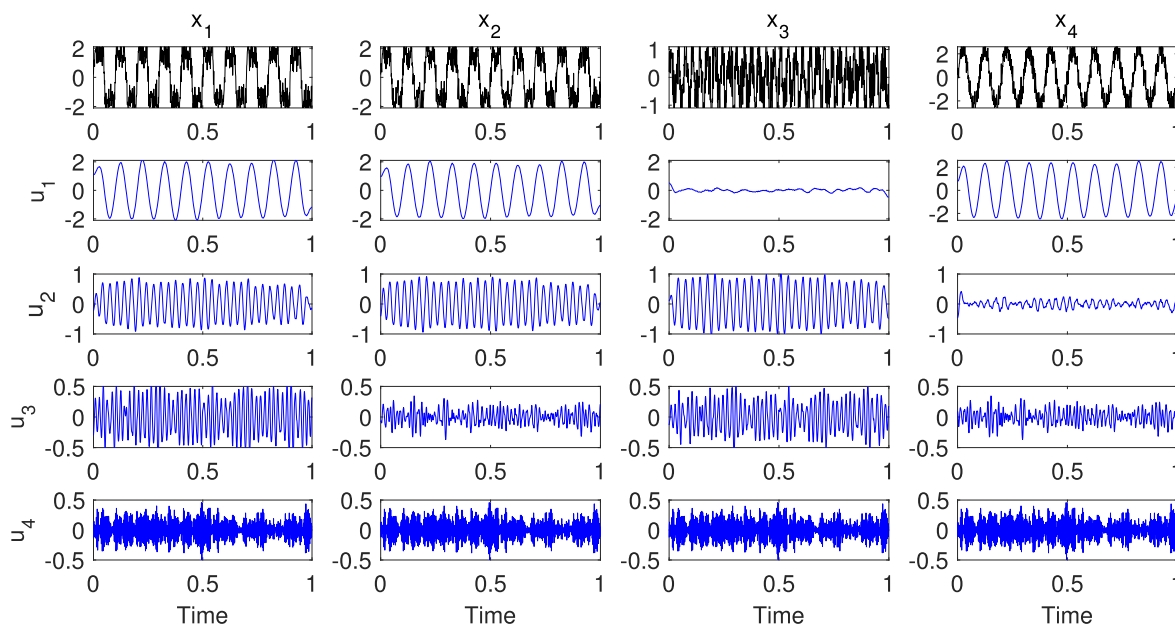

FIGURE 6. The decomposition results of MVMD with $K = 4$, which meets over-decomposition problem [36]. The black line and the blue line represent the input signal and the decomposed signal, respectively.

A. NUMERICAL EXAMPLE

The first example is a four-channel signal (24), which is used to illustrate the excellent decomposition performance of SSA-MVMD.

$$
\begin{cases}
x_1(t) = 2\cos(2\pi \times 10t) + 0.66\cos(2\pi \times 30t) \\
\quad + 0.4\cos(2\pi \times 50t) \\
x_2(t) = 1.9\cos(2\pi \times 10t) + 0.7\cos(2\pi \times 30t) \\
x_3(t) = 0.8\cos(2\pi \times 30t) + 0.3\cos(2\pi \times 50t) \\
x_4(t) = 2.4\cos(2\pi \times 10t)
\end{cases}
\tag{24}
$$

To simulate disturbances, multivariate signal (24) is contaminated by noise $\eta \sim \mathcal{N}(0, 0.1)$. The maximum iteration of SSA is set as $M = 25$, according to reference [29].

Remark 2: We use the signal model (24) *mainly for the following two reasons: (i)* (24) *is multivariate, thus it can simulate the signals sampled from multi-loops. Experiments on this signal can test the decomposition performance of the proposed method for unit-wide oscillations. (ii) This signal model is composed of several higher order harmonics, which is the typical characteristics of nonlinearity-induced oscillations. Therefore, testing on this signal model can effectively simulate the performance of the proposed method in detecting and diagnosing process nonlinearity-induced unit-wide oscillations.*

Figure 2 displays the fitness trend of SSA-MVMD parameter optimization process. It can be observed that the fitness curve shows a trend of gradual convergence. And the
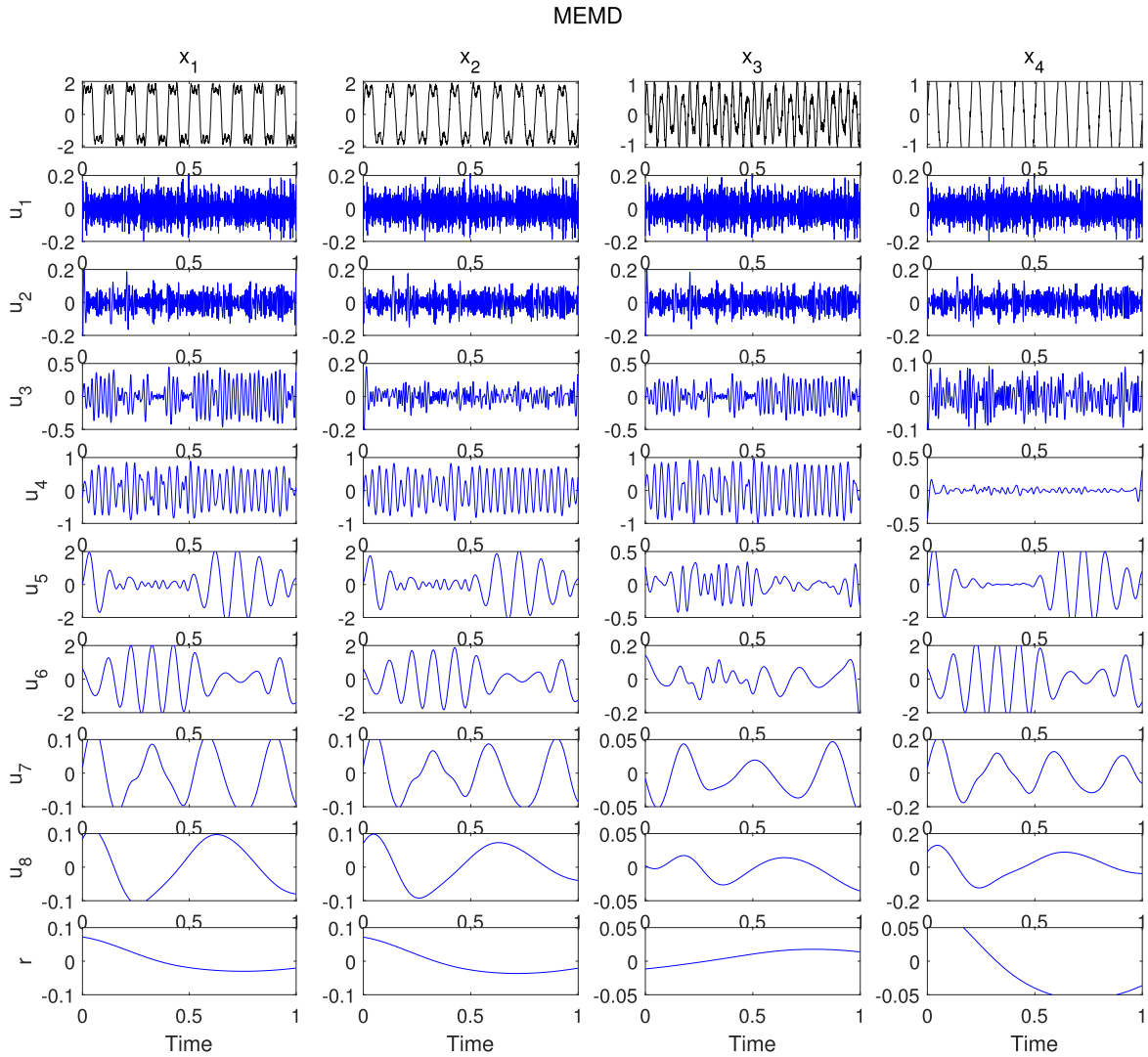
FIGURE 7. The decomposition results of MEMD [20] for signal (24). It can be observed that MEMD is subjected to mode-splitting issue [23].

TABLE 1. The unit-wide oscillation detection and diagnosis results of the simulated control system based on SSA-MVMD.

Variable	Mode	ϖ	ζ	Oscillation?	M_f	Min_f	Max_f	Harmonic	Nonlinearity?
1	u_1	1	0.9263	Yes	0.0167	0.0159	0.0171	1st	
	u_2	0.3875	0.4142	No	-	-	-	1st	No
	u_3	0.0914	0.2268	No	-	-	-	1st	
2	u_1	1	0.9156	Yes	0.0167	0.0159	0.0168	1st	
	u_2	0.3135	0.4369	No	-	-	-	-	No
	u_3	0.1121	0.3966	No	-	-	-	-	
3	u_1	1	0.9487	Yes	0.0167	0.0163	0.0172	1st	
	u_2	0.4211	0.7801	Yes	0.0333	0.0271	0.0338	2rd	Yes
	u_3	0.3129	0.6152	Yes	0.0667	0.0664	0.0711	4th	
4	u_1	1	0.8998	Yes	0.0168	0.0151	0.0207	1st	
	u_2	0.4487	0.7259	Yes	0.0331	0.0295	0.0391	1rd	Yes
	u_3	0.1758	0.2864	No	-	-	-	-	

optimization result reports that the optimal parameter is $K = 3$ and $\alpha = 3144$. The decomposition results of

SSA-MVMD with optimal parameter pairs are presented in Figure 3, in which the blue solid line and the red dotted
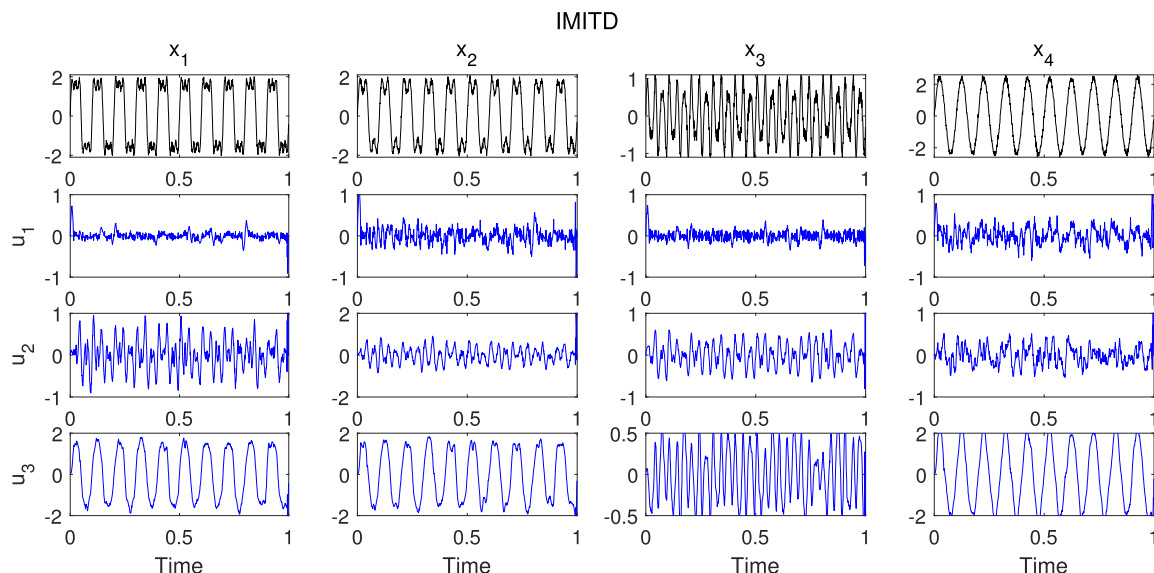
FIGURE 8. The decomposition results of IMITD [25] for signal (24). It can be seen that IMITD suffers from both mode-mixing and end-effect issue [34].
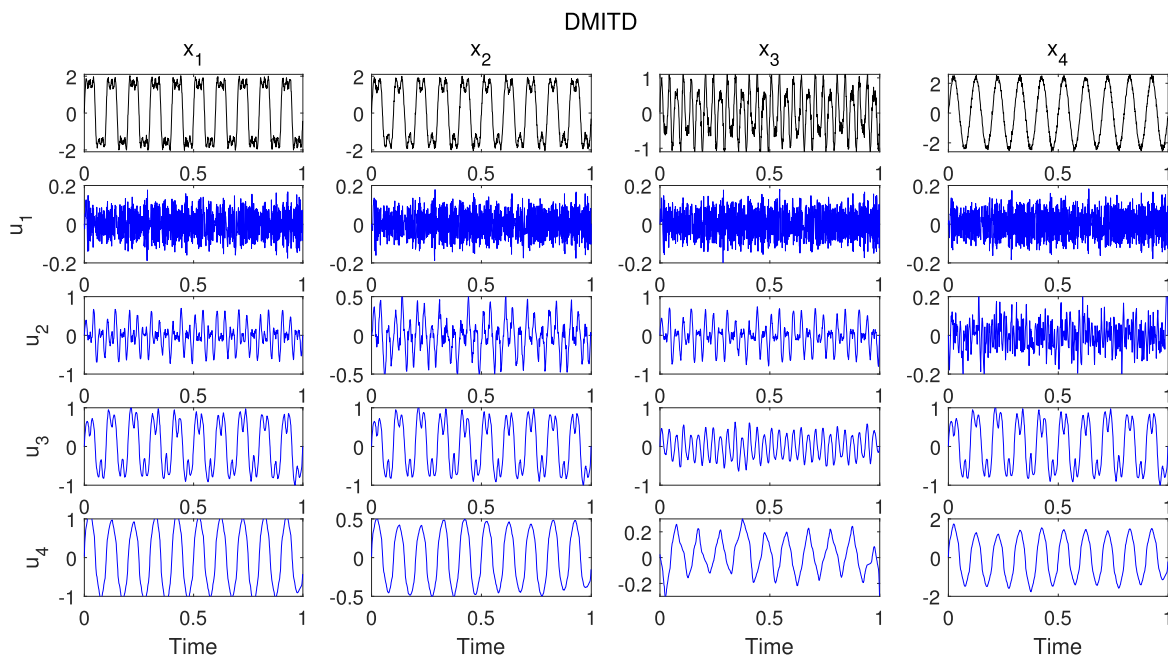

FIGURE 9. The decomposition results of DMITD [25] for signal (24). It is observed that DMITD produces redundant modes and cannot correctly extract modes.

line represent the decomposed mode and the actual mode respectively. The better the coincidence of blue line and red line, the more satisfactory the decomposition performance is. It can be seen from Figure 3 that the all modes are well extracted by SSA-MVMD.

By contrast, Figure 4 provides the decomposition results of MVMD without optimizing the α parameter. The quadratic penalty term α used by the original MVMD method is 500 in Sections IV and V. The modes center frequencies initialization method in MVMD used in Section IV is random. It can

be observed that MVMD encountered difficulties and its performance was relatively poor in this case. Thus, it is inferred that optimizing the α value is very meaningful to improve the MVMD performance. In order to illustrate the influence of mode number K, Figure 5 and 6 display the decomposition results of MVMD with $K = 2$ and $K = 4$, respectively. It can be seen that MVMD shows under-decomposition and over-decomposition issue [36], [37] in Figure 5 and 6, respectively. Therefore, it implies that determining the appropriate mode number is necessary for MVMD to decompose signals
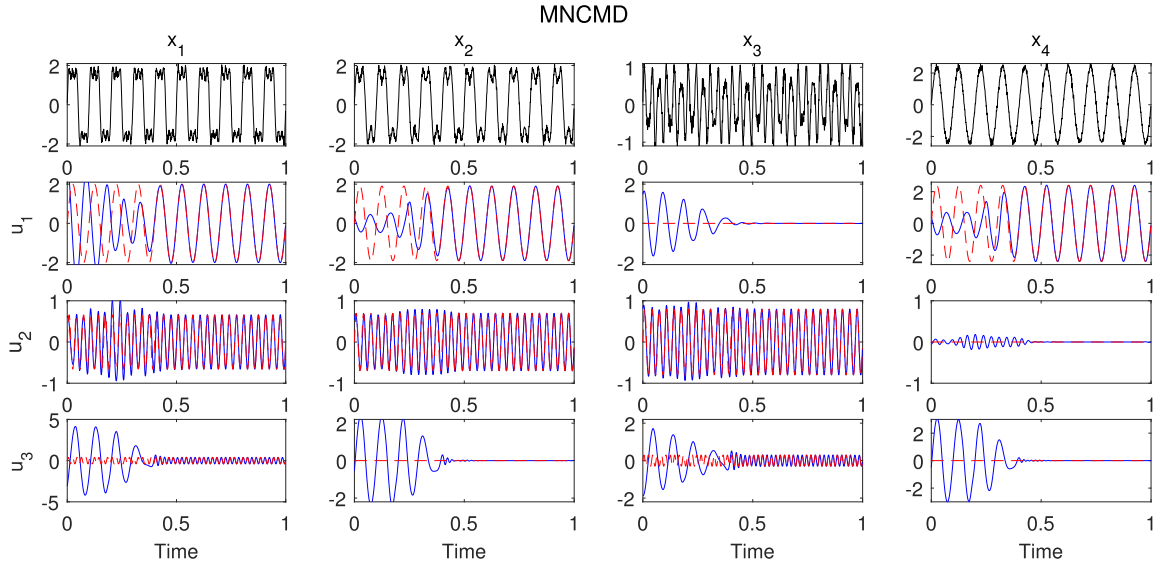
MNCMD

FIGURE 10. The decomposition results of MNCMD. The blue solid line and the red dotted line represent the decomposed mode and the actual mode, respectively. It can be observed that MNCMD suffers from serious mode-mixing issue.

correctly. These comparative experimental results show that the proposed SSA-MVMD effectively improves the decomposition performance of the original MVMD by optimizing the parameter pairs.

The proposed SSA-MVMD also outperforms other classical multivariate signal decomposition methods, such as MEMD [20], IMITD [25], DMITD [26], and MNCMD (multivariate nonlinear chirp mode decomposition) [38]. Figure 7, 8, 9, and 10 shows the decomposition of MEMD, IMITD, DMITD, and MNCMD, respectively. It can be observed that these methods suffer from various difficulties, such as mode-mixing and end-effect issue. To sum up, SSA-MVMD not only outperforms the original MVMD, but also shows more appealing results than MEMD [20], IMITD [25], DMITD [26], and MNCMD [38]. These advantages provide a reliable guarantee for unit-wide oscillation detection and diagnosis in the following experiments.

We use the sum of mean square deviation error to quantify the decomposition performance under different noise sources,

$$error = \sum_{k=1}^{K} \sum_{q=1}^{Q} \sqrt{\frac{\left(u_{k,q}(t) - \tilde{u}_{k,q}(t)\right)^2}{N}} \qquad (25)$$

where $u_{k,q}(t)$ and $\tilde{u}_{k,q}(t)$ are the true mode and estimated mode, respectively. K and Q represent the mode number and channel number, respectively. N is the data length. The noise is $\eta \sim \mathcal{N}(0, \sigma)$. Herein, let σ gradually change from 0 to 0.5 with interval 0.05. The decomposition performance is plotted in Figure 11. It can be observed that the proposed method does not fail until there is a lot of noise. Thus, the proposed method is robust to noise.

In addition, we also test the decomposition performance of the proposed method under colored noise. The colored
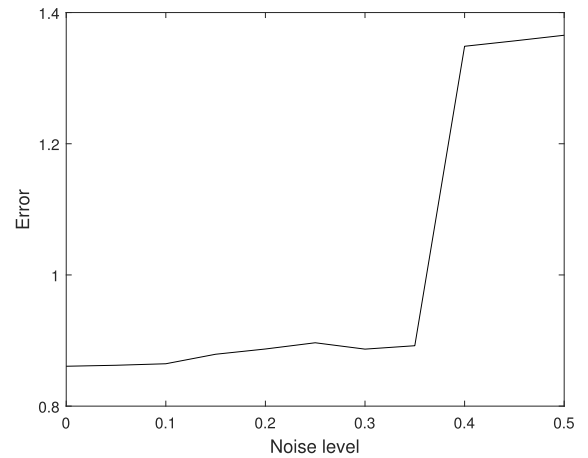

FIGURE 11. The decomposition performance of the proposed method under different noise levels. It can be observed that the proposed method does not fail until there is a lot of noise. Thus, the proposed method is robust to noise.

noise is obtained by passing white noise through the filter $1/\left(1 - 0.7z^{-1}\right)$. The whiter noise follows $\eta \sim \mathcal{N}(0, 0.1)$. The decomposition results of the proposed method are provided in Figure 12. It is observed that the proposed method also maintains good decomposition performance under colored noise.

B. CONTROL SYSTEM
An example control system is developed to test the method presented in this work. The fundamental model of this system is modeled in Simulink [39]. A description of this system is provided here. The chosen example system consists of two tanks. A diagram of the system is shown in Figure 13. The outlet from the tank B flows into the tank A. Each tank has
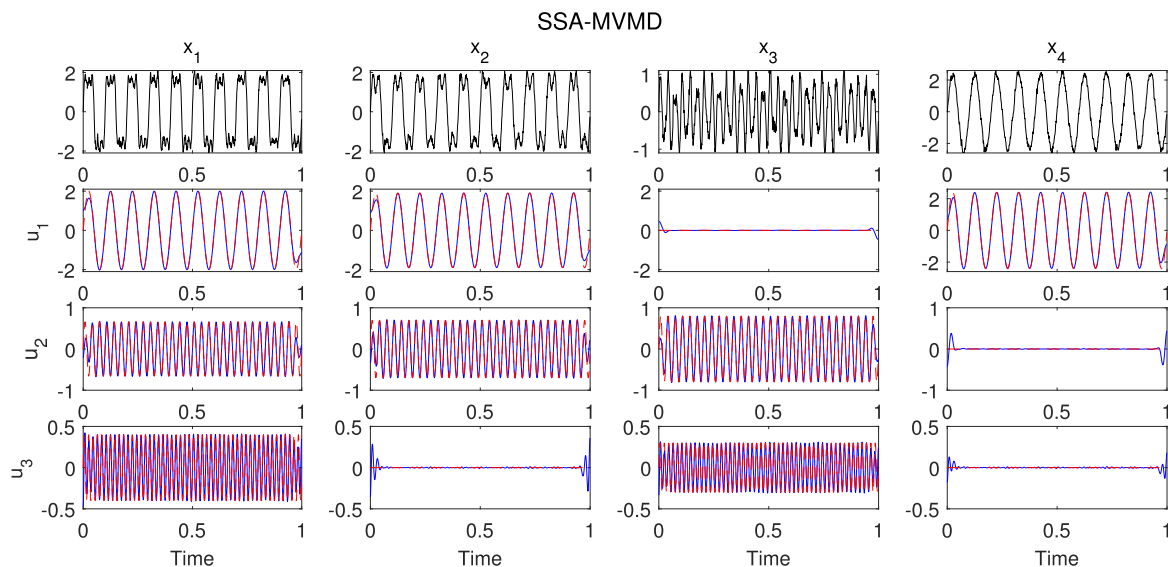
SSA-MVMD

FIGURE 12. The decomposition results of the proposed method under colored noise. The blue solid line and the red dotted line represent the decomposed mode and the actual mode, respectively.
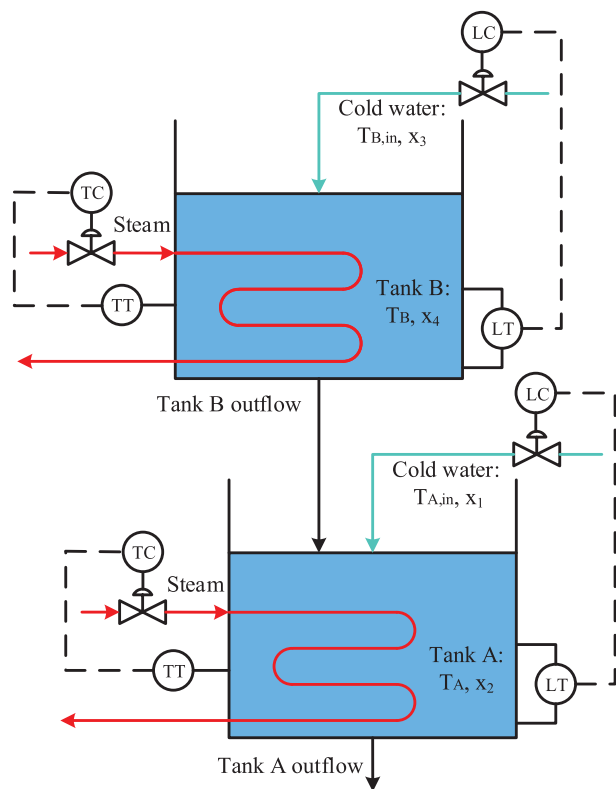

FIGURE 13. Control system structure diagram.

its own supply of cold water with a control valve to control the level of each tank. Each tank also exchanges heat with a steam line. The temperature in the tanks is controlled using the control valves on the steam lines. The controllers used are simple proportional integral derivative (PID) controllers

that change the values of the MVs (manipulated variables) according to the deviation of the controlled variables from their set-points.

The main variables of interest are the temperatures, namely, the inlet temperature of tank A ($T_{A,in}$), the temperature of tank A (T_A), the inlet temperature of tank B ($T_{B,in}$), and the temperature of tank B (T_B). The unit of temperature is Celsius. These data have been standardized, so the unit annotation is omitted. For convenience, there four variables are noted as x_1, x_2, x_3, and x_4, respectively. In this experiment, a valve-nonlinearity problem is introduced into the control loop where the inlet temperature of tank B $T_{B,in}$ (x_3) is located. Due to the valve-nonlinearity problem, the whole control system shows a unit-wide oscillation, which can be observed in the first row of Figure 14.

Herein, the SSA-MVMD is applied to the multivariate signal $\mathbf{x}(t) = [x_1(t), x_2(t), x_3(t), x_4(t)]$ and the corresponding decomposition results are displayed in Figure 14. The corresponding oscillation detection indicators are listed in Table 1. To intuitively represent the detection results, Figure 15 visualizes the modes satisfying the oscillation conditions $\varpi_{k,q} > \widehat{\varpi}$ and $\zeta_{k,q} > \widehat{\zeta}$ in Figure 14. The black blocks in Figure 15 correspond to the oscillating modes in Figure 14. It can be observed from Figure 14 and 15 that both x_1 and x_2 only contains one oscillating mode. Therefore, only the first harmonic exists in these two variables. And the oscillation of these two variables is unlikely to be caused by nonlinearity. Both x_3 and x_4 displays higher order harmonics according to Algorithm 3, thus the unit-wide oscillation is induced by nonlinearity problem. Note that the different parts of a unit tend to behave as low pass mechanical filters and thus filter out the higher harmonics as we move away from the source of nonlinearity [30]. Because the harmonic order of x_3 is higher, it is more probable to be the source of the
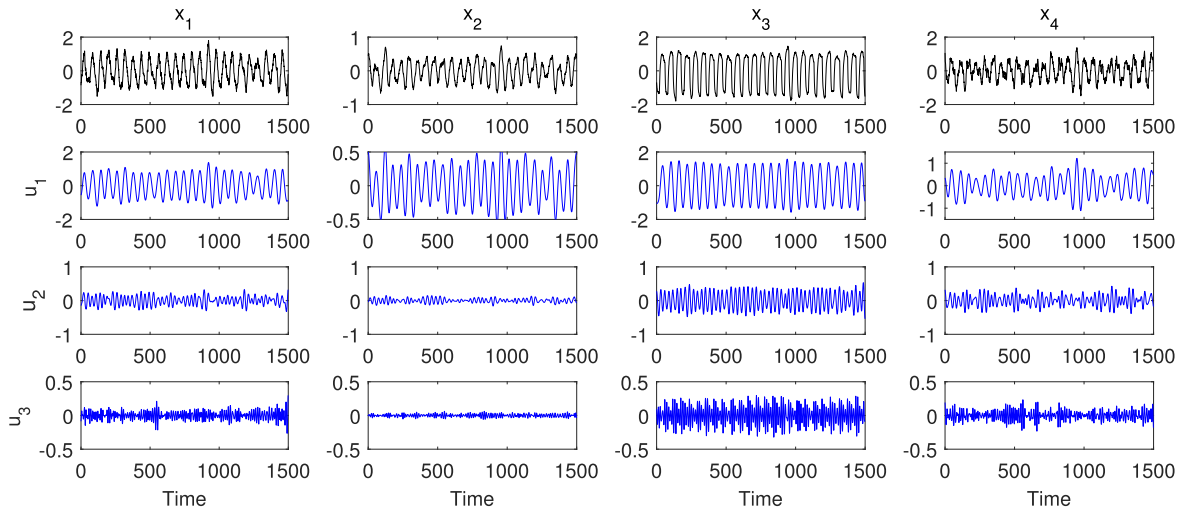
FIGURE 14. The process variables (the first row) and decomposition results obtained from SSA-MVMD of the unit-wide oscillations.
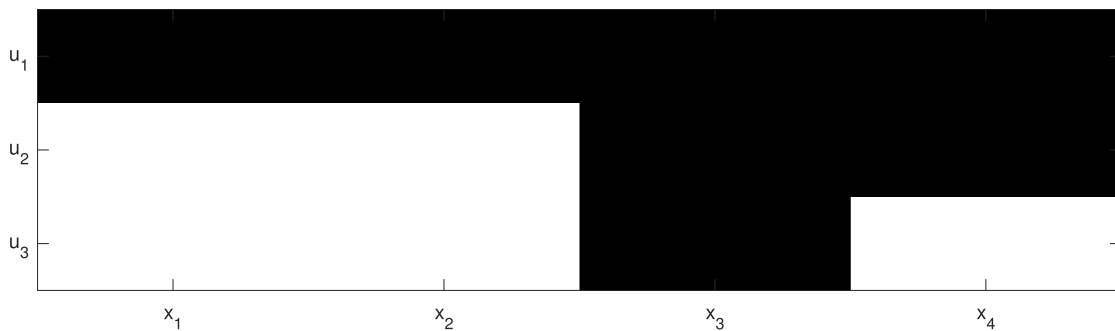

FIGURE 15. Visualization of oscillation detection indicators. These black blocks correspond to the oscillating modes in Figure 14, which satisfy the conditions $\varpi_{k,q} > \widehat{\varpi}$ and $\zeta_{k,q} > \widehat{\zeta}$.
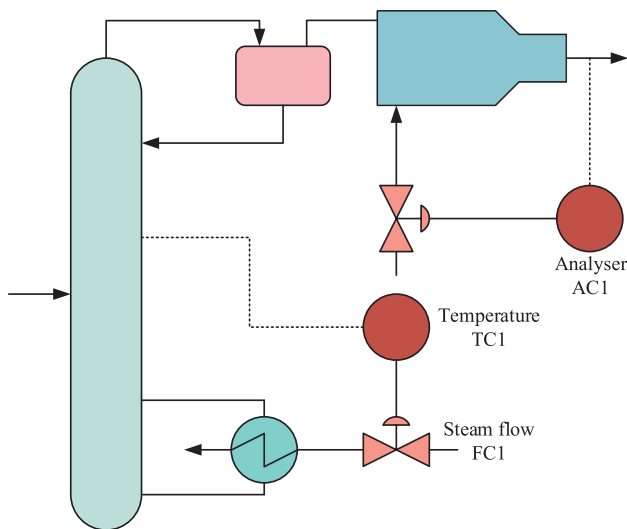

FIGURE 16. Industrial refinery separation unit diagram. This system showed a unit-wide oscillation in the distillation column.

nonlinearity-induced unit-wide oscillations. This conclusion conforms to the predefined settings. Therefore, it can be

concluded that the proposed method is able to detect and diagnose the nonlinearity-induced unit-wide oscillations.

V. INDUSTRIAL CASES

The industrial case study concerns the chemical process [40]. The data are from an Australian refinery separation unit, whose diagram is shown in Figure 16. The sampling interval is 20 s. The data set includes the analyser AC1, steam flow FC1, and temperature TC1 measurements. These data have been standardized, so the unit annotation is omitted. For convenience, this work records these three variables AC1, FC1, and TC1 as x_1, x_2, and x_3 respectively.

During production, the operator found that this system showed a unit-wide oscillation in the distillation column. The time trend of the analyser indicates the composition of the product leaving the top of column was varying in an undesirable behavior. Through a full analysis and research, it is known that the there was a nonlinearity fault in the steam flow loop FC1. It was an orifice plate flow meter but there was no weep-hole in the plate which had the effect that condensate collected on the upstream side until it reached a critical level, and the accumulated liquid would then periodically clear itself by siphoning through the orifice [41]. The challenge for
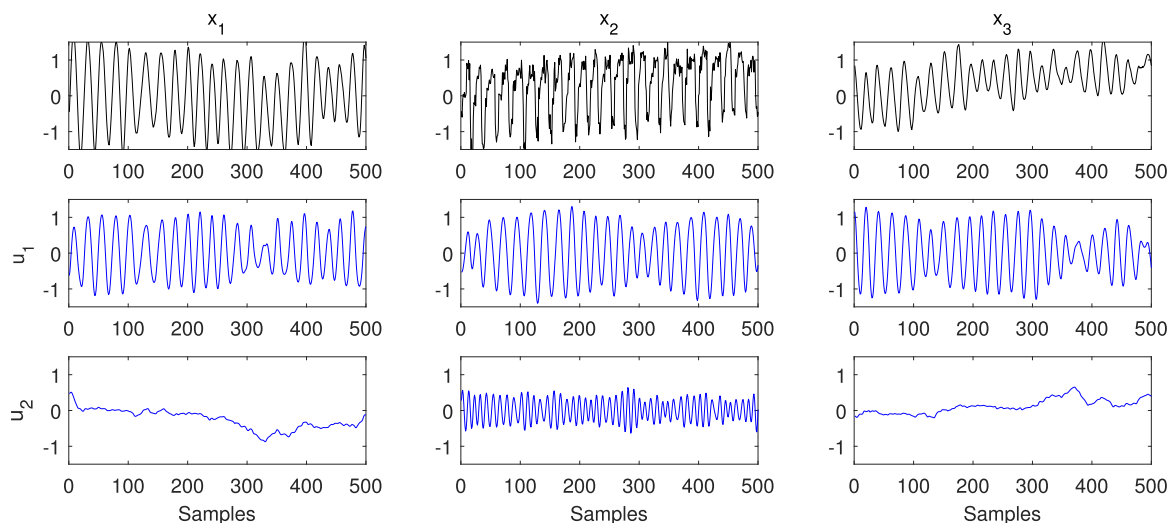
FIGURE 17. The process variables (the first row) and decomposition results obtained from SSA-MVMD of the industrial unit-wide oscillations.
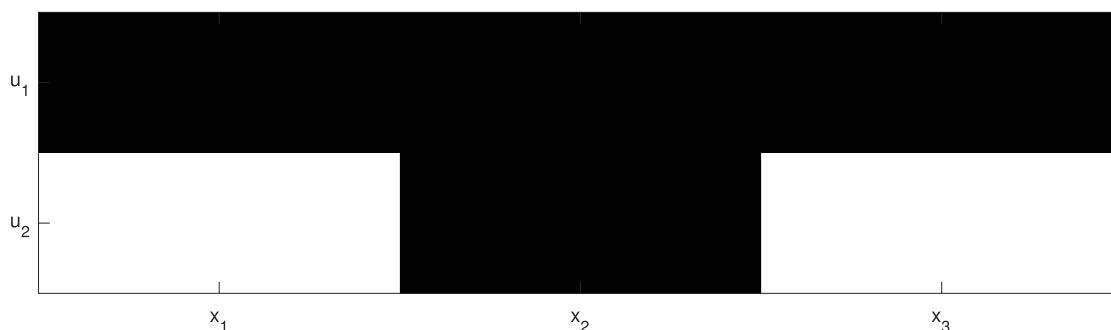

FIGURE 18. Visualization of oscillation detection indicators of industrial case. These black blocks correspond to the oscillating modes in Figure 17, which satisfy the conditions $\varpi_{k,q} > \widehat{\varpi}$ and $\zeta_{k,q} > \widehat{\zeta}$.

TABLE 2. The unit-wide oscillation detection and diagnosis results of the industrial refinery separation unit.

Variable	Mode	ϖ	ζ	Oscillation?	M_f	Min_f	Max_f	Harmonic	Nonlinearity?
1	u_1	1	0.8411	Yes	0.0024	0.0159	0.0171	1st	No
	u_2	0.1107	0.3965	No	-	-	-	-	
2	u_1	1	0.8303	Yes	0.0025	0.0023	0.0026	1st	Yes
	u_2	0.4657	0.7920	Yes	0.0048	0.0047	0.0051	2rd	
3	u_1	1	0.7866	Yes	0.0024	0.0163	0.0172	1st	No
	u_2	0.0964	0.4010	No	-	-	-	-	

the analysis of this system is to verify that the nonlinearity faulty steam flow loop is the root cause of the unit-wide oscillations [4].

Figure 17 provides the process variables of these three loops in the first row. The corresponding decomposition results of SSA-MVMD are shown in the subgraphs of the second and third rows in blue lines. The details of detection and diagnosis are listed in Table 2. For visualization, the corresponding detection results are visualized in Figure 18, where the black block represents the oscillation mode. It can be clearly seen from Table 2 and Figure 18 that except the

second variable x_2 contains higher harmonics, all other variables have only first harmonics. According to Algorithm 3, the oscillations contained in x_2 are nonlinearity-induced oscillations. And the reason for the oscillation of variables x_1 and x_3 is that the nonlinearity-induced oscillation of x_2 propagates to these loops, causing the unit-wide oscillations. In addition, the loop where the second variable is located can be considered to be closer to the unit-wide oscillation source, because the harmonic contained in x_2 has the highest order. The detection and diagnosis results are completely consistent with the ground truth [41].
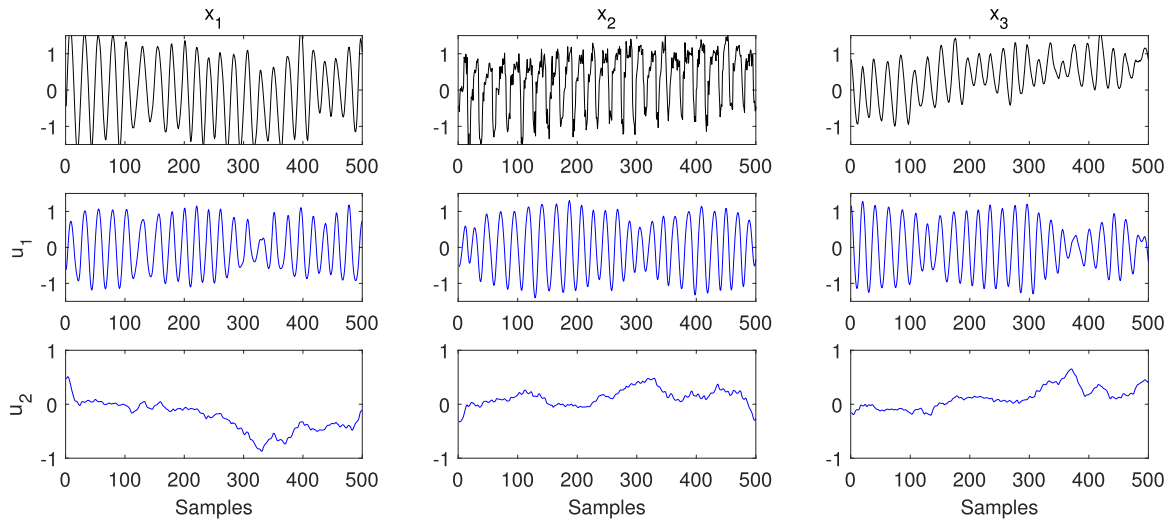
FIGURE 19. The process variables (the first row) and decomposition results obtained from the original MVMD of the industrial unit-wide oscillations. It is clear that the original MVMD does not extract the higher order harmonics contained in variable x_2. Thus, it cannot correctly detect and diagnose the nonlinearity-induced unit-wide oscillations.
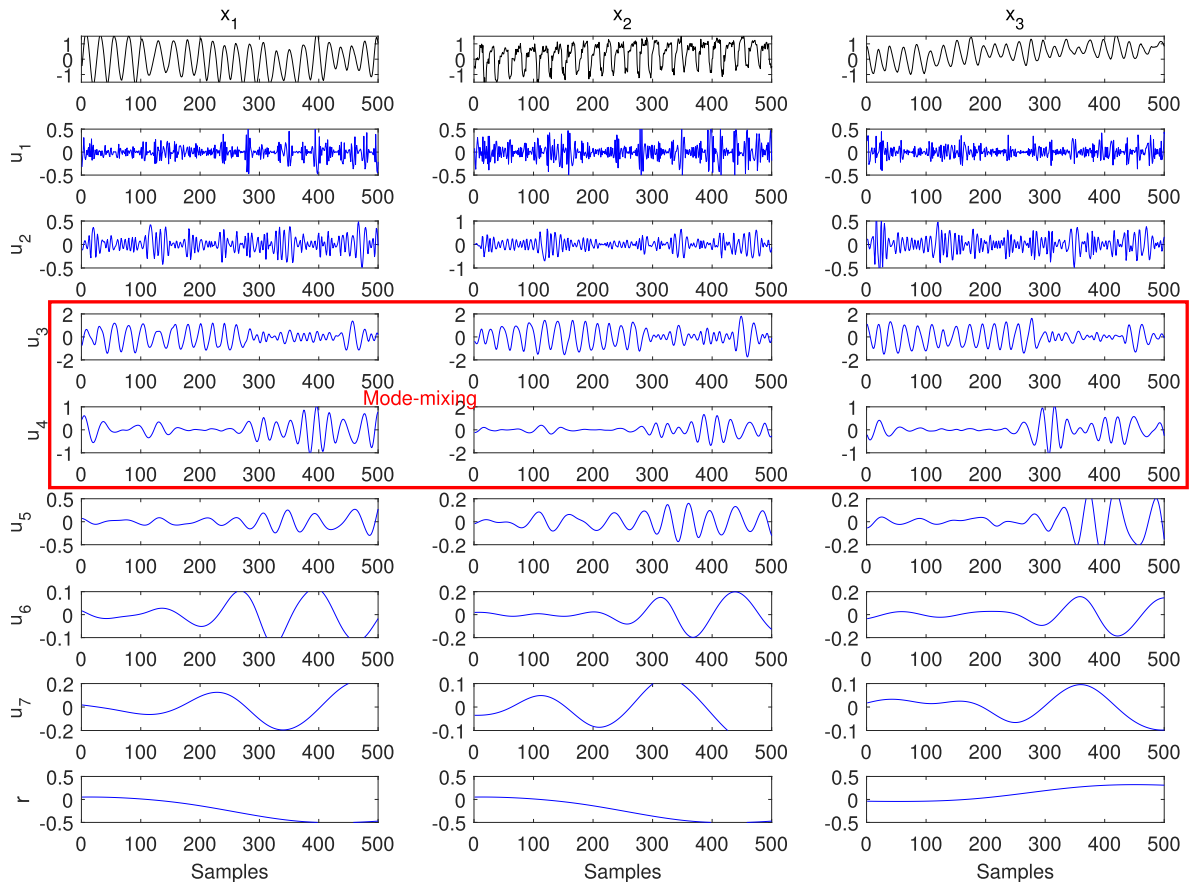

FIGURE 20. The process variables (the first row) and decomposition results obtained from MEMD of the industrial unit-wide oscillations. The mode-mixing issue is apparent, which will degrade the detection and diagnosis performance of unit-wide oscillations.

In order to highlight the advantages of the proposed method, the original MVMD- and MEMD-based methods [17], [21] are applied to this industrial case. Figure 19 shows the decomposition results of original MVMD [17]. It can be seen from Figure 19 that the original MVMD does not completely extract the second order harmonic

contained in the unit-wide oscillation, which will result in failure to diagnose nonlinearity problem. With respective to the MEMD-based method [21], Figure 20 indicates that MEMD not only produces too many redundant modes, but also encounters serious mode-mixing issue, which will lead to the distortion of oscillation frequency. Therefore, it can be concluded that the proposed outperforms the original MVMD and MEMD-based methods [17], [21] in detecting and diagnosing the unit-wide oscillations in real industrial environment.

VI. CONCLUSION

An SSA-MVMD algorithm is proposed to solve the parameter pair optimization problem of the original MVMD. Experimental results show that SSA-MVMD algorithm is not only better than the original MVMD, but also outperforms the classical MEMD [20], IMITD [25], DMITD [26], and MNCMD [38] algorithms. Following, based on the SSA-MVMD, a nonlinearity-induced unit-wide oscillation detection and diagnosis method is proposed. The SSA-MVMD-based detector combines the normalized correlation coefficient and sparseness index to detect the significant oscillating modes. Then, the presence of nonlinearity problem can be identified through investigating the frequency relationship among these modes. In the end, the effectiveness and advantages of the proposed method are demonstrated by a series of simulations as well as industrial cases. Compared with the latest related works [17], [21], this work shows better decomposition performance, thus providing more reliable and accurate detection results. Therefore, it can be concluded that the proposed method shows great potential values for control performance assessment and monitoring.

In the future, we would like to apply the proposed method to detect and diagnose more types of process oscillations, such as those caused by the controller.

REFERENCES

[1] J. W. Dambros, J. O. Trierweiler, and M. Farenzena, "Oscillation detection in process industries—Part I: Review of the detection methods," *J. Process Control*, vol. 78, pp. 108–123, Jun. 2019.

[2] M. Jelali and B. Huang, *Detection and Diagnosis of Stiction in Control Loops: State of the Art and Advanced Methods*. Berlin, Germany: Springer, 2009.

[3] Q. Chen, J. Chen, X. Lang, L. Xie, C. Jiang, and H. Su, "Diagnosis of nonlinearity-induced oscillations in process control loops based on adaptive chirp mode decomposition," in *Proc. Amer. Control Conf. (ACC)*, Jul. 2020, pp. 2772–2777.

[4] Q. Chen, X. Fei, L. Xie, D. Li, and Q. Wang, "Causality analysis in process control based on denoising and periodicity-removing CCM," *J. Intell. Manuf. Special Equip.*, vol. 1, no. 1, pp. 25–41, Dec. 2020.

[5] M. F. Aftab, M. Hovd, and S. Sivalingam, "Diagnosis of plant-wide oscillations by combining multivariate empirical mode decomposition and delay vector variance," *J. Process Control*, vol. 83, pp. 177–186, Nov. 2019.

[6] T. Hägglund, "A control-loop performance monitor," *Control Eng. Pract.*, vol. 3, no. 11, pp. 1543–1551, 1995.

[7] K. Forsman and A. Stattin, "A new criterion for detecting oscillations in control loops," in *Proc. Eur. Control Conf. (ECC)*, Aug. 1999, pp. 2313–2316.

[8] T. Miao and D. E. Seborg, "Automatic detection of excessively oscillatory feedback control loops," in *Proc. IEEE Int. Conf. Control Appl.*, vol. 1, Aug. 1999, pp. 359–364.

[9] T. I. Salsbury and A. Singhal, "A new approach for ARMA pole estimation using higher-order crossings," in *Proc., Amer. Control Conf.*, Jun. 2005, pp. 4458–4463.

[10] H. Cui, Y. Guan, H. Chen, and W. Deng, "A novel advancing signal processing method based on coupled multi-stable stochastic resonance for fault detection," *Appl. Sci.*, vol. 11, no. 12, p. 5385, 2021.

[11] Z.-H. Zhang, F. Min, G.-S. Chen, S.-P. Shen, Z.-C. Wen, and X.-B. Zhou, "Tri-partition state alphabet-based sequential pattern for multivariate time series," *Cognit. Comput.*, vol. 18, no. 12, pp. 1–19, May 2021.

[12] R. Srinivasan, R. Rengaswamy, and R. Miller, "A modified empirical mode decomposition (EMD) process for oscillation characterization in control loops," *Control Eng. Pract.*, vol. 15, no. 9, pp. 1135–1148, Sep. 2007.

[13] L. Xie, X. Lang, J. Chen, A. Horch, and H. Su, "Time-varying oscillation detector based on improved LMD and robust Lempel–Ziv complexity," *Control Eng. Pract.*, vol. 51, pp. 48–57, Jun. 2016.

[14] Z. Guo, L. Xie, T. Ye, and A. Horch, "Online detection of time-variant oscillations based on improved ITD," *Control Eng. Pract.*, vol. 32, pp. 64–72, Nov. 2014.

[15] L. Xie, X. Lang, A. Horch, and Y. Yang, "Online oscillation detection in the presence of signal intermittency," *Control Eng. Pract.*, vol. 55, pp. 91–100, Oct. 2016.

[16] Q. Chen, X. Lang, L. Xie, and H. Su, "Detecting nonlinear oscillations in process control loop based on an improved VMD," *IEEE Access*, vol. 7, pp. 91446–91462, 2019.

[17] N. U. Rehman and H. Aftab, "Multivariate variational mode decomposition," *IEEE Trans. Signal Process.*, vol. 67, no. 23, pp. 6039–6052, Dec. 2019.

[18] Q. Chen, X. Lang, L. Xie, and H. Su, "Multivariate intrinsic chirp mode decomposition," *Signal Process.*, vol. 183, Jun. 2021, Art. no. 108009.

[19] X. Lang, D. Zhong, L. Xie, and J. Chen, "Application of improved multivariate empirical mode decomposition to plant-wide oscillations characterization," in *Proc. 6th Int. Symp. Adv. Control Ind. Processes (AdCONIP)*, May 2017, pp. 601–606.

[20] N. Rehman and D. P. Mandic, "Multivariate empirical mode decomposition," *Proc. Roy. Soc. A, Math., Phys. Eng. Sci.*, vol. 466, no. 2117, pp. 1291–1302, 2010.

[21] M. F. Aftab, M. Hovd, and S. Sivalingam, "Plant-wide oscillation detection using multivariate empirical mode decomposition," *Comput. Chem. Eng.*, vol. 117, pp. 320–330, Sep. 2018.

[22] N. Rehman, C. Park, N. E. Huang, and D. P. Mandic, "EMD via MEMD: Multivariate noise-aided computation of standard EMD," *Adv. Adapt. Data Anal.*, vol. 5, no. 2, 2013, Art. no. 1350007.

[23] X. Lang, Q. Zheng, Z. Zhang, S. Lu, L. Xie, A. Horch, and H. Su, "Fast multivariate empirical mode decomposition," *IEEE Access*, vol. 6, pp. 65521–65538, 2018.

[24] X. Lang, Y. Zhang, L. Xie, X. Jin, A. Horch, and H. Su, "Use of fast multivariate empirical mode decomposition for oscillation monitoring in noisy process plant," *Ind. Eng. Chem. Res.*, vol. 59, no. 25, pp. 11537–11551, Jun. 2020.

[25] X. Lang, Z. Zhang, L. Xie, A. Horch, and H. Su, "Time-frequency analysis of plant-wide oscillations using multivariate intrinsic time-scale decomposition," *Ind. Eng. Chem. Res.*, vol. 57, no. 3, pp. 954–966, 2018.

[26] X. Lang, Q. Zheng, L. Xie, A. Horch, and H. Su, "Direct multivariate intrinsic time-scale decomposition for oscillation monitoring," *IEEE Trans. Control Syst. Technol.*, vol. 28, no. 6, pp. 2608–2615, Nov. 2020.

[27] J. Zhang, X. Xu, Q. Chen, L. Xie, and H. Su, "Extracting fetal heart rate from abdominal ECGs based on fast multivariate empirical mode decomposition," in *Proc. 16th Int. Conf. Control, Autom., Robot. Vis. (ICARCV)*, Dec. 2020, pp. 648–653.

[28] R. G. da Silva, M. H. Dal Molin Ribeiro, N. Fraccanabbia, V. C. Mariani, and L. dos Santos Coelho, "Multi-step ahead bitcoin price forecasting based on VMD and ensemble learning methods," in *Proc. Int. Joint Conf. Neural Netw. (IJCNN)*, Jul. 2020, pp. 1–8.

[29] J. Xue and B. Shen, "A novel swarm intelligence optimization approach: Sparrow search algorithm," *Syst. Sci. Control Eng.*, vol. 8, no. 1, pp. 22–34, Jan. 2020.

[30] N. F. Thornhill, S. L. Shah, and B. Huang, "Detection of distributed oscillations and root-cause diagnosis," *IFAC Proc. Volumes*, vol. 34, no. 27, pp. 149–154, 2001.

[31] J. M. Lilly and S. C. Olhede, "Analysis of modulated multivariate oscillations," *IEEE Trans. Signal Process.*, vol. 60, no. 2, pp. 600–612, Feb. 2012.

[32] X. Lang, B. He, Y. Zhang, Q. Chen, and L. Xie, "Adaptive clutter filtering for ultrafast Doppler imaging of blood flow using fast multivariate empirical mode decomposition," in *Proc. IEEE Int. Ultrason. Symp. (IUS)*, Sep. 2021, pp. 1–4.

[33] Q. Chen, J. Chen, X. Lang, L. Xie, N. Rehman, and H. Su, "Self-tuning variational mode decomposition," *J. Franklin Inst.*, vol. 358, no. 15, pp. 7825–7862, 2021.

[34] Q. Chen, J. Chen, X. Lang, L. Xie, S. Lu, and H. Su, "Detection and diagnosis of oscillations in process control by fast adaptive chirp mode decomposition," *Control Eng. Pract.*, vol. 97, Apr. 2020, Art. no. 104307.

[35] N. Thornhill, S. Shah, and B. Huang, "Detection and diagnosis of unit-wide oscillations," *Process Control Instrum.*, vol. 26, no. 4, pp. 26–28, Jul. 2000.

[36] K. Dragomiretskiy and D. Zosso, "Variational mode decomposition," *IEEE Trans. Signal Process.*, vol. 62, no. 3, pp. 531–544, Feb. 2014.

[37] Q. Chen, X. Lang, Y. Pan, Y. Shi, L. Xie, and H. Su, "Detecting multiple plant-wide oscillations in process control systems based on multivariate intrinsic chirp component decomposition," in *Proc. CAA Symp. Fault Detection, Supervision, Saf. Tech. Processes (SAFEPROCESS)*, Dec. 2021, pp. 1–6.

[38] Q. Chen, L. Xie, and H. Su, "Multivariate nonlinear chirp mode decomposition," *Signal Process.*, vol. 176, Nov. 2020, Art. no. 107667.

[39] Q. Chen, X. Lang, S. Lu, N. U. Rehman, L. Xie, and H. Su, "Detection and root cause analysis of multiple plant-wide oscillations using multivariate nonlinear chirp mode decomposition and multivariate Granger causality," *Comput. Chem. Eng.*, vol. 147, Apr. 2021, Art. no. 107231.

[40] Q. Chen, X. Xu, Y. Shi, X. Lang, L. Xie, and H. Su, "MNCMD-based causality analysis of plant-wide oscillations for industrial process control system," in *Proc. Chin. Autom. Congr. (CAC)*, Nov. 2020, pp. 5617–5622.

[41] N. F. Thornhill and A. Horch, "Advances and new directions in plant-wide disturbance detection and diagnosis," *Control Eng. Pract.*, vol. 15, no. 10, pp. 1196–1206, 2007.

ZHULIANG LIN received the B.S. degree in industrial automation education and the M.S. degree in control theory and control engineering from the Zhejiang University of Technology, Hangzhou, China, in 1998 and 2009, respectively. He is currently an Associate Professor with the Xingzhi College, Zhejiang Normal University. His current research interests include control science and control engineering.

MIN SUN received the B.S. degree in automation from Zhejiang Sci-Tech University, Hangzhou, China, in 2007. He is currently a Control Engineer in Zhejiang Kende Mechanical and Electrical Company Ltd., Taizhou. His research interest includes process control technology.
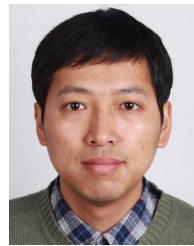
XIALAI WU received the B.S. degree in automation from Zhejiang Sci-Tech University, China, in 2007, and the Ph.D. degree in control science and engineering from Zhejiang University, China, in 2019. He is currently a Lecturer at Huzhou University. His current research interests include process control, signal processing, and integrated design and control.

● ● ●